C. R. Geoscience 342 (2010) 653–667

Contents lists available at ScienceDirect

Comptes Rendus Geoscience

www.sciencedirect.com

Geochemistry

Geochemical modelling of fluid–rock interactions in the context of the Soultz-sous-Forêts geothermal system

Modélisation géochimique des interactions fluides–roches dans le contexte du système géothermique de Soultz-sous-Forêts

Bertrand Fritz [a,*], Emmanuel Jacquot [a,b], Benoit Jacquemont [a], Armelle Baldeyrou-Bailly [a], Michel Rosener [a,c], Olivier Vidal [d]

[a] *Laboratoire d'hydrologie et de géochimie de Strasbourg (LHYGES), UMR 7517, université de Strasbourg, CNRS, 1, rue Blessig, 67084 Strasbourg cedex, France*
[b] *Geokemex sarl, 18, rue Alain-Savary, 25000 Besançon, France*
[c] *Geodynamics Ltd, PO BOX 2046, Milton QLD 4064, Australia*
[d] *Observatoire des sciences de l'univers Grenoble (LGCA), UMR 5025, université J.-Fourier, CNRS, 1381, rue de la Piscine, BP 53, 38041 Grenoble cedex, France*

ARTICLE INFO

Article history:
Received 16 June 2009
Accepted after revision 1 February 2010
Available online 10 April 2010

Written on invitation of the Editorial Board

Keywords:
Water–Rock interactions
Geochemical modelling
Experimental approach
Enhanced Geothermal System (EGS)
Soultz-sous-Forêts (France)

Mots clés :
Interactions fluides–roches
Modélisation géochimique
Approche expérimentale
Système géothermique stimulé
Soultz-sous-Forêts (France)

ABSTRACT

The development of the Enhanced Geothermal System (EGS) at Soultz-sous-Forêts (France) has given to scientists an interesting opportunity for the application of geochemical modelling of water–rock interactions, combining theoretical studies with field and experimental data. The main results of four successive and complementary studies are summarized: geochemical modelling of fluid–rock interactions with prediction of dissolution/precipitation of minerals, feed-back effects on the mineralogy and petrography of the rock (major role of silicates in the geological past and of carbonates in the near future of the exploitation), experimental control of the dynamics of silicates under thermal gradient and relation between the evolution of the petrophysics of the rocks and the heat and mass transfers. The thermal cycle of the fluid, between 200 °C and 65 °C in the geothermal loop, may be responsible for dissolution/precipitation of minerals which modify the porosity and permeability of the granite, as it happened in the geological past, in relation with hydrothermal circulations in the Rhine Graben.

RÉSUMÉ

Le développement du projet de géothermie profonde à Soultz-sous-Forêts (France) sur le concept de Système Géothermique Stimulé (en anglais : *Enhanced Geothermal System* – EGS) a fourni aux scientifiques une très intéressante opportunité pour l'application de la modélisation géochimique des interactions fluides–roches en combinant les études théoriques aux données de terrain et d'expérimentations. Les principaux résultats de quatre études successives et complémentaires sont synthétisés : modélisation des interactions fluides–roches avec prévision des dissolutions/précipitations de minéraux et effets en retour sur la minéralogie et la pétrographie des roches (rôle majeur des silicates dans le passé géologique et des carbonates au début de la future exploitation géothermique), test expérimental de la dynamique des silicates sous gradient thermique,

* Corresponding author.
E-mail addresses: bfritz@illite.u-strasbg.fr (B. Fritz), emmanuel.jacquot@geokemex.eu (E. Jacquot), abailly@unistra.fr (A. Baldeyrou-Bailly), michel.rosener@geodynamics.com.au (M. Rosener), olivier.vidal@ujf-grenoble.fr (O. Vidal).

1631-0713/$ – see front matter © 2010 Académie des sciences. Published by Elsevier Masson SAS. All rights reserved.
doi:10.1016/j.crte.2010.02.005

et finalement relation entre l'évolution pétrophysique des roches et les transferts de masse et de chaleur dans le réservoir. Le cycle thermique du fluide, entre 200 °C et 65 °C, peut être à l'origine de dissolutions/précipitations de minéraux, ce qui peut modifier la porosité et la perméabilité du granite, comme cela s'est produit, dans le passé géologique, en relation avec les circulations hydrothermales dans le graben rhénan.

1. Introduction

The prediction of the possible evolution of the granitic rock at the Soultz-sous-Forêts EGS site has been a real challenge for scientists. The rock will be submitted to the circulation of the geothermal fluid, initially present in the granite depth (mainly between 3.5 and 5 km) at thermodynamic equilibrium with the rock-forming minerals, pumped in the production wells (temperature up to 200 °C), exploited for heat and power production in the surface installation and finally re-injected in the geothermal reservoirs after cooling in the surface heat exchanger (temperature down to 60–65 °C). In this thermal loop the fluid–rock system will be out of equilibrium compared to what it was in the deep reservoir: some minerals may dissolve, some others may precipitate and this will modify the porosity and the permeability of the rock.

The paper is organized as follows. In section 1 we summarize the results of a modelling approach of these processes (Durst, 2002; Jacquot, 2000) related to the first period of circulation tests on the EGS type geothermal site, when the Soultz system was only drilled down to 3.6 km depth. This modelling showed the importance of carbonates on short term in the system. In Section 2, we mention the results of a petrographic study and associated modelling for the past evolution of the geological system focused on mass transfers, particularly of silicates on long term. In Section 3 we report on some experimental approach of these fluid–rock interactions under a strong thermal gradient with an important dynamics of silicates in these conditions. Section 4 makes the relation between the petrophysical study of the granite in the geothermal systems and the numerical modelling of the effect of heat transfers.

2. Fluid–rock interactions in the geothermal cycle: thermodynamic and kinetic modelling (Jacquot, 2000)

The geothermal context

In 1997, the European EGS site at Soultz-sous-Forêts has been experimented for important production tests in order to demonstrate that it was possible to impose the circulation of a thermal fluid through the fractured granitic rock at great depth (> 3.5 km), maintaining a fluid production between 20 l/s and 100 l/s in one or two production wells. In 1997 the geothermal fluid was extracted from the granitic reservoir through the production well at 3876 m, at more than 140 °C. This produced fluid was cooled at 65 °C in order to simulate the thermal energy exploitation, and this cooled fluid was re-injected in the granitic reservoir at the injection well at 3590 m depth where the horizontal distance between the two wells was 500 m. This distance is particularly high compared to other geothermal systems in the world and is one of the Soultz EGS challenges: temperature up to 200 °C in the final design of the project, depth of wells around 5 km, distance between wells feet around 500 m. The circulation tests were conducted with a stabilized rate of injection/pumping during 4 months. On the industrial point of view, the aim was to predict the long term evolution of the transport properties of the exploited geothermal reservoir and the geochemical risks associated to possible dissolutions and/or precipitations of minerals in the fractures network in the granite.

A first geochemical modelling approach was based on a thermodynamic and kinetic modelling of water–rock interactions using the code KINDIS (Madé et al., 1994a, 1994b) in order to simulate the major steps of the fluid–granite interactions. The aim was to simulate the possible hydrothermal fluid–rock interactions which may occur in the geothermal reservoir during such a test period and during a future long term exploitation in comparable conditions. The first step of the study has been to define a modelling strategy adapted to a real case in order to obtain quantitative estimations of the geochemical fluid–rock interaction processes, mainly dissolutions and precipitations of minerals.

This is described here from Jacquot (2000). The first stage of the study was to define the "initial" state of the reservoir, before any injection or circulation. The next step was to evaluate the geochemical thermodynamic disequilibrium states induced by the circulation of a fluid which is re-injected at a lower temperature than the reservoir temperature and with a chemical composition which may differ from the chemistry of the fluid in the reservoir. These chemical disequilibrium states may induce an evolution of the geothermal reservoir, particularly because porosity and permeability are concerned by minerals dissolution/precipitation processes.

2.1. Interpretation of the initial state of the system

The petrography and mineralogy of the granitic rock at Soultz-sous-Forêts have been intensively studied (Genter, 1989; Genter and Traineau, 1992, 1996; Genter et al., 1995, 1997; Ledésert et al., 1993a, 1993b; Sardini et al., 1997; Traineau et al., 1991). The mineralogy of the three major rock facies is presented in Fig. 1. The petrographic observations showed that the natural hydrothermal alteration of the granitic rock corresponds to a significant dissolution of K-spar and plagioclases, associated with precipitation of quartz, clay minerals (mainly illites and smectites) and carbonates (calcite and dolomite).

The hydrothermal fluids which did generate in the geological past these mineralogical transformations are of

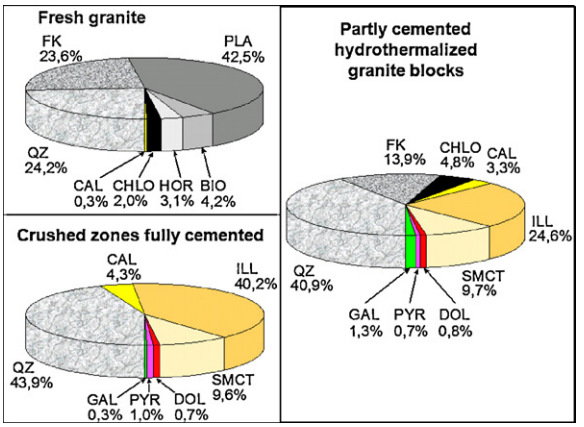

Fig. 1. Quantitative mineralogy (volume %) of the three main facies of the granitic basement on the Soultz-sous-Forêts EGS site. ILL = illite; SMCT = smectite; CAL = calcite; DOL = dolomite; PYR = pyrite; GAL = galena.

Fig. 1. Composition minéralogique (% en volume) de trois faciès majeurs du granite du socle du site EGS de Soultz-sous-Forêts ILL = illite ; SMCT = smectite ; CAL = calcite ; DOL = dolomite ; PYR = pyrite ; GAL = galène.

Table 1
Composition of the hydrothermal fluid at 3500 m depth and 165 °C calculated at thermodynamic equilibrium with mineral phases of the partly cemented hydrothermalized granite blocks facies.

Tableau 1
Composition du fluide hydrothermal à 3500 m de profondeur et 165 °C, calculée à l'équilibre thermodynamique avec les phases minérales du granite hydrothermalisé, partiellement cimenté.

Element	Molality (mMol/kg H_2O)
Na	1190
Ca	166
K	65.5
Mg	4.17
Si	1.80
Fe	0.116
Al	7.44 E-03
Pb	0.035 E-03
Cl	1580
S	3.22
F	0.171
pH	4.8
Alkalinity	15 meq kg^{-1}
Eh	−245 mV

course unknown. The fluids extracted today are not very easy to characterize as in situ-conditions at depth. It is of course impossible to avoid some evolution between reservoir conditions and lab conditions:

- reequilibration with atmospheric conditions: dissolution of atmospheric oxygen with strong evolution of redox conditions after extraction and sampling;
- strong temperature evolution between about 165 °C at depth and 20 °C in the lab with unavoidable CO_2 degassing and consequent evolutions of pH (increase), alkalinity (decrease if carbonate precipitates), as shown by several authors (Aquilina et al., 1997; Komninou and Yardley, 1997; Pauwels et al., 1992, 1993).

Geochemical modelling allows, however, to better interpret these evolutions in order to define the in situ conditions. The numerical code KINDIS (Madé, 1991; Madé et al., 1994a, 1994b) has been applied considering the analytical results obtained on the collected fluids. The model is used to define the composition of a geothermal fluid in equilibrium with the granitic rock whose mineralogy has been described in details (primary and secondary minerals) at 165 °C and for a pH value of 4,8, measured during the 1997 circulation tests directly in the fluid circulating in the pumping pipes without being in contact with atmosphere. The calculations allow defining, in particular, the in situ chemical variables which are not precisely determined in the lab because of the possible evolution after sampling (Al, Fe^{2+}, Fe^{3+}, Eh, alkalinity, total inorganic carbon). The recalculated composition of the fluid is given in Table 1.

The thermal exchanger at surface creates in the fluid a rapid cooling between 165 and 65 °C. If one supposes that no significant mineral precipitations occur during this rapid cooling (Jacquot, 2000), the major concentrations of elements in the extracted fluid are almost the same at 60–65 °C compared to their value at 165 °C, and the fluid goes from a quasi equilibrium state with minerals at 165 °C in the reservoir to a disequilbrium state at 60 °C as shown by the saturation indexes of the minerals of interest (Fig. 2).

The large over-saturations predicted for galena and pyrite are in good accordance with observations made in the circulating fluid out of the heat exchanger during the 1997 circulation tests. Metallic sulfides may precipitate rapidly from these oversaturated fluids as described by Rickard (Rickard, 1988, 1995).

2.2. Simulation of the geochemical evolution of the reservoir during exploitation

After cooling, the geothermal fluid oversaturated with respect to several minerals (Fig. 2) is re-injected in the fractures network of the granitic body, where it circulates from the injection well to the production well where it is re-heated between 60 °C and about 165 °C.

In order to be able to predict the geochemical evolution of the fluid along this process, it is necessary to apply a model which integrates kinetic rate laws for minerals. The numerical code KINDIS (Madé, 1991; Madé et al., 1994a, 1994b) allows such an approach but does not include the thermal evolution in a given run: it runs at a fixed temperature up to 300 °C. This is, of course, a limitation in the direct modelling approach when the fluid is supposed to heat progressively like in the geothermal reservoir for the re-injected fluid at Soultz. In order to take this into account, a successive sequence of simulations has been done with isothermal calculation steps every ten degrees. At each step temperature all thermodynamic conditions were recalculated for chemical speciation and minerals solubilities and the fluid–rock interaction consequences

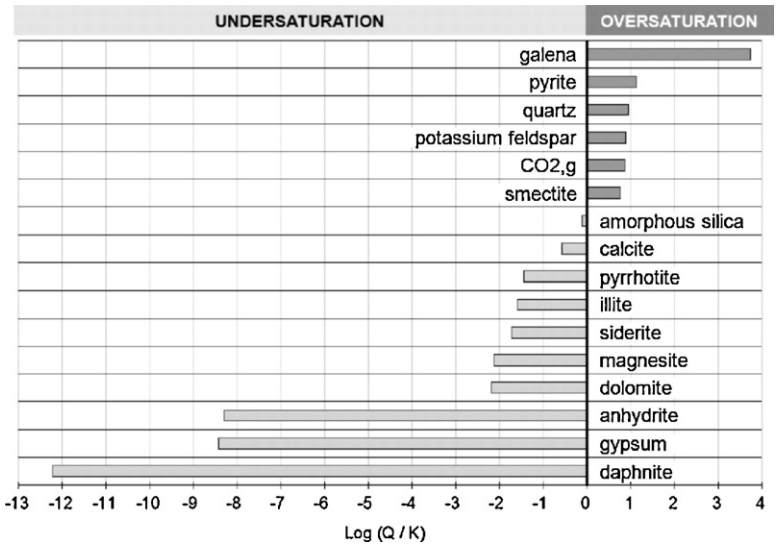

Fig. 2. Saturation indexes of minerals in the hydrothermal fluid after instantaneous cooling down to 60 °C at the outlet of the heat exchanger of the EGS of Soultz-sous-Forêts (Q is the ion activity product and K is the thermodynamic equilibrium constant of the mineral hydrolysis reaction).

Fig. 2. Indices de saturation des minéraux dans le fluide hydrothermal après refroidissement instantané à la sortie de l'échangeur thermique du système. EGS de Soultz-sous-Forêts (Q est le produit ionique d'activité, K est la constante d'équilibre thermodynamique pour la réaction d'hydrolyse du minéral).

were predicted. The sequence of 10 simulations between 60 °C and 160 °C is represented in Fig. 3 versus time.

Among the different petrographic facies in the Soultz granite (Fig. 1) the so-called hydrothermalized granite is mainly concerned by the circulation of injected fluids because of its high permeability as compared to the "fresh" granite and to the so called "crushed zones" which are totally cemented.

For the simulation this facies was therefore the only one considered for the evolution of physical properties of the reservoir. The results of the modelling of the sequence of

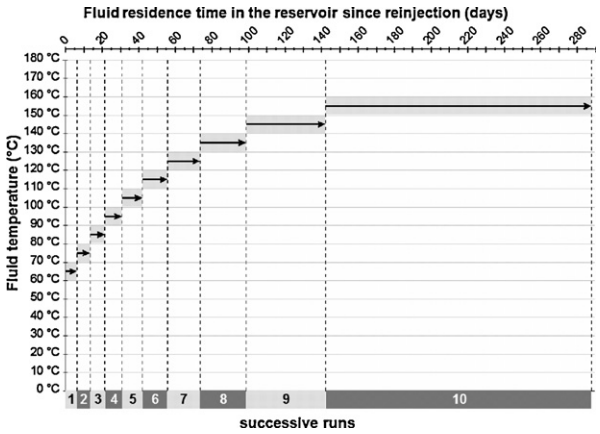

Fig. 3. Modelling strategy developed to give an account of water–rock interactions and hydrothermal fluid temperature increase within the stimulated geothermal reservoir of the EGS at Soultz-sous-Forêts during the summer 1997 circulation test.

Fig. 3. Stratégie de modélisation géochimique, développée pour rendre compte des interactions eau–roche et de la montée en température du fluide hydrothermal dans le système EGS de Soultz-sous-Forêts au cours des tests de circulation de l'été 1997.

dissolution and precipitation processes are given in Fig. 4 as a function of the progressive temperature increase of the fluid.

For each of the ten successive simulations, as steps of increasing temperature, the volumic balance between dissolved and precipitated minerals has been calculated, in order to detect the tendency of the system to open or close the fracture network of the geothermal reservoir. This is strongly related to different behaviours of carbonate and silicate minerals. The volumic balance of silicates is essentially controlled by quartz, K-spar and the hydrated magnesium-rich smectite. Despite their abundance in contact with the hydrothermal fluid in the fractures of the granitic body, the contribution of silicates to the volumic balance of dissolved and precipitated minerals remains very small. Therefore, the dissolution of dolomite and the precipitation of calcite explain the major part of the evolution of the porosity in the geothermal reservoir during the exploitation as shown in Fig. 5. The major part of the volume of minerals dissolved or precipitated concerns these carbonates.

If carbonates alone represent the main part of the mineral volumic change, despite their minor abundance in the granitic rock reacting with the hydrothermal fluid (less than 5% of the exchange surface between rock and fluid), this is due to the difference of reactivity between silicates and carbonates, the latter being several order of magnitude more rapid to dissolve or precipitate, as an example seven orders of magnitude at 25 °C and near neutral pH values (e.g. White et al., 1999). Even if the exchange surface between the fluid and the carbonates is two orders of magnitude smaller than the corresponding surface for silicates, the amount of calcite dissolved for a given amount of fluid, and for a given time duration, is five orders of magnitude higher than for silicates.

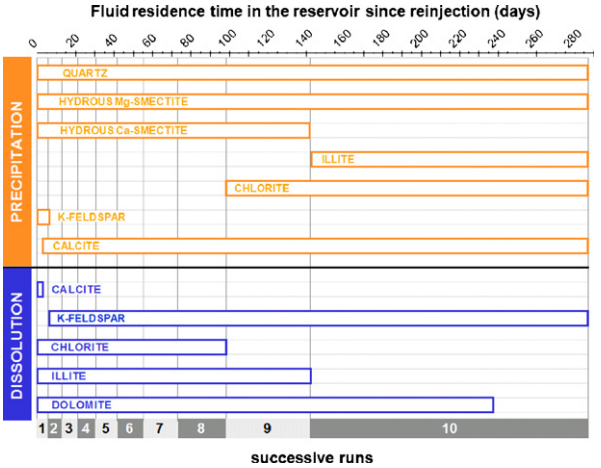

Fig. 4. Qualitative sequence of dissolution and precipitation processes occurring within the geothermal reservoir during the re-heating of the re-injected geothermal fluid as simulated for the summer 1997 circulation test on the Soultz-sous-Forêts EGS.

Fig. 4. Séquence qualitative simulée des processus de dissolution et précipitation se produisant dans le réservoir géothermal, durant le réchauffement du fluide géothermal réinjecté dans le système EGS de Soultz-sous-Forêts, au cours des tests de circulation de l'été 1997.

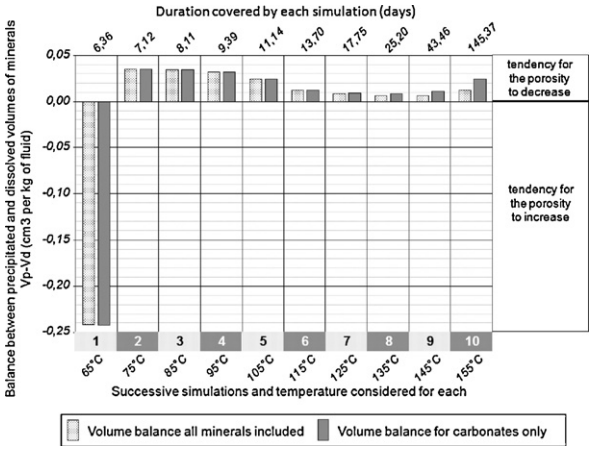

Fig. 5. Volumic balance between dissolution and precipitation of minerals for the successive simulations at increasing temperature.

Fig. 5. Bilan volumique entre dissolution et précipitation de minéraux pour les simulations successives de montée en température.

2.3. Discussion of the modelling

These geochemical simulations show clearly that even if the re-injected cooled hydrothermal fluid is able to produce smectites with swelling properties, the evolution of the reservoir porosity is essentially controlled by the carbonate phases. This is due to the fact that the dissolution or precipitation kinetics of carbonates are very fast compared to those of silicates: even if silicates represent 95% of the volume of the granite submitted to the induced hydrothermal alteration, they only play a minor role in the evolution of the porosity on short term during the re-injection tests (several months). On the contrary, initial minor carbonates in the rock play an essential role in controlling the evolution of the porosity and therefore the permeability, a key-point for the future long-term evolution of the geothermal system. However, neglecting the effect of silicates dissolution/precipitation is only a first approximation valid for short-term processes and experimental results document this problem for long-term reactions (Oelkers et al., 1994; Sausse et al., 2001; Vidal, 1997; Vidal and Durin, 1999). Developing a kinetic model for the precipitation of secondary clay phases in alteration processes (Fritz et al., 2009) is important for being able to predict the long term processes that will take place in the fractures of the geothermal reservoir at Soultz-sous-Forêts, or having occurred in the past on a geological time scale.

Another limitation of this first modelling is related to the fact that the KINDIS code is not a coupled transport–reaction model and the formation of secondary phases was not located in space, in the geothermal reservoir. However, the qualitative result on carbonates and silicates (batch type approach) has been confirmed (Durst, 2002; Portier and Vuataz, 2010) using a more complex modelling approach combining fluid–rock interactions and heat and fluid transport, showing that calcite and dolomite, compared to quartz and pyrite, presented the maximum potential for precipitation or dissolution. These authors showed that a significant dissolution of carbonates should occur in the re-injection zone while re-precipitation should occur later in the re-injection path in the reservoir. This was obtained using the code FRACHEM, a 2D simplified reservoir model (Durst, 2002).

In these coupled models, like KIRMAT (Gérard et al., 1998), which are often applied on small metric size systems like clay barriers in nuclear waste storages systems (Marty, 2006; Marty et al., 2010), the challenge is now to document kinetic data bases for complex clay phases (dissolution and precipitation), particularly from experimental approaches as will be presented later in this study.

3. Palaeo fluid–rock interactions in the granitic body: quantification and modelling of mass transfers

The simulation of the fluid composition evolution during the short-term tests of the reservoir detected the possible formation of carbonates, silicates being formed mainly on long term. For the future geothermal exploitation it is important to predict how the system will be concerned by long-term processes. It appeared therefore interesting to see what had been registered in the reservoir during palaeo-thermal alterations. This could be done from the petrographic study of the core material extracted from drillings. The information from palaeo-mass transfers which can be detected in the altered granite is a good indicator of what can be expected during the future exploitation.

The Soultz-sous-Forêts granitic batholith is an interesting example of a system where past and actual fluid circulations along fracture have induced mineralogical and chemical transformations in the granitic basement and in the overlying terrains. The quantification of the mass

transfers which resulted in the granite from successive hydrothermal circulations has been studied at temperatures ranging from 120 °C to 350 °C (Jacquemont, 2002). This approach was done after an accurate petrographic description of the various alteration facies from 800 m of Soultz's granite core samples using the Gresens method of mass transfers quantification (Gresens, 1967; Potdevin and Marquer, 1987). This method aims to determine the behaviour of chemical elements during alteration and to establish alteration mass balance at three different levels, i.e., the mineralogical reactions, the alteration horizons and the whole granite body.

The results show that titanium and aluminium are immobile elements at the mineral grain level. Calcium, manganese, iron and magnesium appear to be widely exchanged through the different facies but remain somewhat stable at the scale of the entire granitic body. Silicium, potassium and sodium transfers are noticed at the various scales. Moreover silica and potassium contributions originating from sedimentary fluids were demonstrated. Sodium coming from plagioclase alteration concentrated in the solutions and could have been exported out of the system.

The results of the mass balance calculations on the core samples show that elemental transfers were essentially localized in the fractured zones where illitic alteration took place as a consequence. This alteration is characterized by an intense rock hydrolysis. The replacement of the primary minerals by tiny clay crystals enhances the porosity increase in the granite. Compared to unaltered rock, highly illitized granites are characterized by lower densities and rather constant volume that indicates a mass decrease as compared to the parental rock. In the heart of the fractured zones, the granite is often cemented by quartz and calcite. Such secondary mineral precipitations induce a porosity decrease, and an increase of the rock mass compared to the highly illitized facies.

A geochemical modelling of the fluid–rock interactions has been carried out and showed that the hydrothermal circulation in an initially fractured and unaltered granite of a fluid with a chemical composition close to that of the present-day fluid in the reservoir could explain the mineralogical compositions observed in the different alteration facies (Jacquemont, 2002). In a quantitative manner, the kinetic modelling over a 1000 years simulated period confirmed that plagioclase alteration into illite was the most important alteration process. The high porosity of the illitized granites could be explained by taking into account the width of the fractures in the model of the physical evolution of the system.

This approach was interesting as compared to the previous one because it concerns, in cores observations, the very long term processes, at geological time scale, and in that case the mass transfers concern mostly the silicates dynamics: carbonates are active on short term but the closed system in the granitic body is not open to CO_2: when short term reactions with carbonates are back to equilibrium, the long term reaction may only concern silicates. This is an indication that geochemical modelling of the long term behaviour of fluid–rock systems in the reservoir should describe accurately the kinetics of silicates precipitation, which is still not very easy with clay-type minerals (Marty et al., 2010; Vidal, 1997) for which new models for nucleation and growth are still under development (Fritz et al., 2009) and need complementary experimental validation. We have developed one type of approach of this problem in the 100–300 °C temperature domain as will be described in the next section.

4. Experimental approach of fluid–rock interactions: the stability of phyllosilicates in a strong thermal gradient

If the dynamics of silicates is the major concern for long-term behaviour of the reservoir, the precipitation of silicates, and particularly of clay minerals, has to be well documented in order to validate the geochemical models combining thermodynamic and kinetic properties of the mineral phases for predicting their long term dynamics in the geothermal system. While numerous experimental studies (Oelkers et al., 1994) focused on the dissolution kinetics, there are not many studies on the precipitation of newly formed phases, because this is generally not easy to detect in short term reactions, particularly for low temperature processes. If strong thermal gradients are expected the mineral evolution and associated mass transport can be studied experimentally with the 'tube-in-tube' design as used by Goffé et al. (1987), Robert and Goffé (1993), Vidal (1997), Vidal and Durin (1999), Vidal et al. (1995). We have developed such an experiment where the starting products are enclosed in a capsule with drilled walls located at one end of a long tube (10 cm) containing only water at the beginning of the experiment and placed in a thermal gradient. During these experiments (Baldeyrou et al., 2003), the starting products dissolve and the aqueous species diffuse toward the opposite end of the tube. Depending on the variation of the mineral solubility with temperature, saturation is achieved and new phases are observed precipitating in the tube, which was free of solids at the beginning of the experiment. Using a powdered granite as starting material, it was shown (Baldeyrou et al., 2003) that albite, orthose and sometimes saponite were observed precipitating at the hot extremity of the tube (300 °C), whereas interlayered illite/smectite and/or dioctahedral smectites were observed with quartz at the cold extremity. Complementary experiments were conducted with different starting assemblages, fluid compositions or temperature ranges.

4.1. Experimental setting and methods

The experiments were conducted either with a powdered granite or with separated phases in the molar proportions given in Fig. 6. The granite is a fine-grained granite from the Flamanville area (France), which has a composition similar to the Soultz-sous-Forêts granite (Baldeyrou-Bailly, 2003). About 20 mg of the starting products were sealed in a gold capsule with drilled walls, which enables the exchange of dissolved species but not of solids. The capsule was placed at the hot extremity of a 10 cm long, 4 mm diameter gold tube filled with 1.5 ml bidistilled water (H_2O) or with a brine similar to the

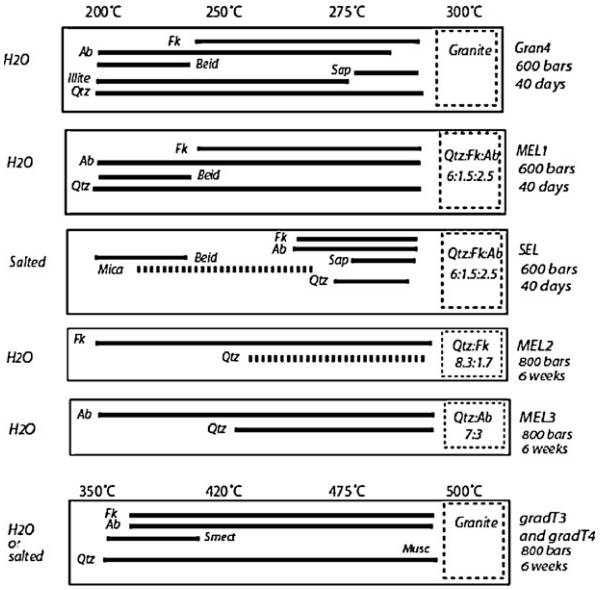

Fig. 6. Experimental results of the tube-in-tube experiments under a thermal gradient. The boxes with dashed outlined represent the capsules containing the starting material (the numbers are molar proportions). The nature of the fluid is indicated on the left side. The bars show the range of temperature were the corresponding newly-formed phases were observed.

Fig. 6. Résultats des expériences de type « *tube-in-tube* » sous gradient thermique. Les boîtes en pointillés représentent les capsules contenant le matériel initial (les nombres représentent les proportions molaires). La nature du fluide est indiquée sur le côté gauche. Les barres indiquent le domaine de température où les phases néoformées ont été observées.

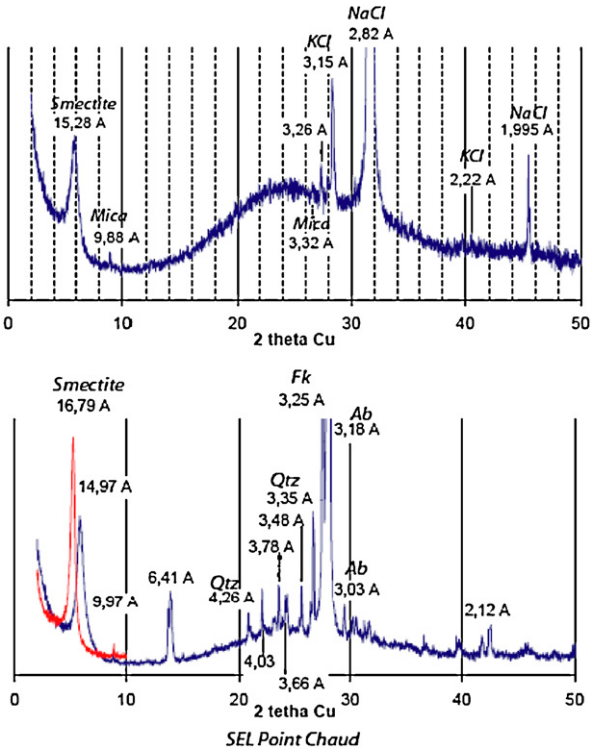

Fig. 7. XRD pattern of the run products in the experiment "SEL". The diagram after ethylene glycol treatment is in red.

Fig. 7. Diagrammes de diffraction des rayons X pour les produits obtenus lors de l'expérience « SEL ». Le diagramme obtenu après traitement à l'éthylène glycol est figuré en rouge.

Table 2
Composition (mMol/Kg H_2O) of the salted fluid used in the experiments SEL and gradT4 (see Fig. 6).

Tableau 2
Composition (mMol/Kg H_2O) du fluide salin utilisé dans les expériences SEL et gradT4 (voir Fig. 6).

Na	Ca	K	Mg	SiO_2	Cl	Al	Fe
1134	147.7	95.1	3.92	6.48	1590	1	2

Soultz-sous-Forêt brine at depth (Aquilina et al., 1997; Pauwels et al., 1993) (Table 2). The welded shut tube was placed in a horizontally oriented cold seal autoclave, with the cold extremity in contact with ambient air and the other extremity in the oven. At the end of the run, the gold tube was removed from the autoclave and immerged in liquid nitrogen in order to freeze the solution, and thus to avoid any displacement of the newly formed phases. The tube containing the freezed water was heated to 80 °C (12 h) to evaporate the solution, and the walls of the tube were observed with a scanning electron microscope (SEM). When possible, the products were collected after the SEM observations for XRD or TEM characterization.

4.2. Experimental results

The experimental conditions and results are shown in Fig. 6, together with the results of Baldeyrou-Bailly (2003), Baldeyrou-Bailly et al. (2004) (experiments Gran4 and MEL1). In all experiments, between 30% (MEL2 and MEL3) and 70% of the starting material was removed from the capsules, which indicates the very efficient mineral–fluid interactions and mass transport within the tube. Most of the newly-formed products were concentrated at the cold extremity of the tube and enough material was generally available for XRD characterization. The amount of solid crystallizing in the middle part of the tube was much lower, but SEM observation and analysis were generally possible.

The nature of the precipitating phases was determined by XRD and by SEM observation and analysis (see Baldeyrou-Bailly (2003) for the experiments Gran4 and MEL1). Figs. 7 and 8 show examples of XRD and micrographs from the SEL experiment at the cold and hot extremities. The occurrence of smectites is indicated by their typical morphologies under the SEM (Fig. 8) and by the presence of XRD peaks at about 15 Å, which are shifted at 16.8 Å after ethylene-glycol treatment (Fig. 7 lower part). The composition of the smectites is plotted in Fig. 9: most compositions at the cold extremities plot close to the beidellite end-member, and few compositions, intermediate between saponite and K-spar (mixed analyses), were obtained at the hot extremity. In the middle part of the tube, the analyses plot either close to K-spar or intermediate between K-spar and sylvite + halite (mechanical

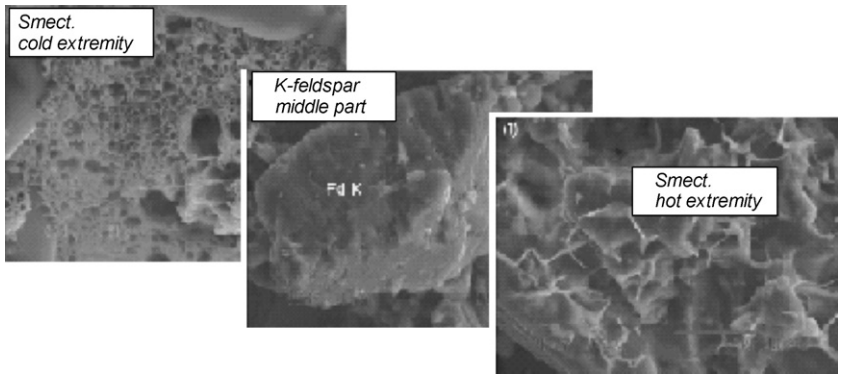

Fig. 8. SEM micrograph of the run products from the experiment "SEL".

Fig. 8. Enregistrement au MEB des produits minéraux obtenus dans l'expérience « SEL ».

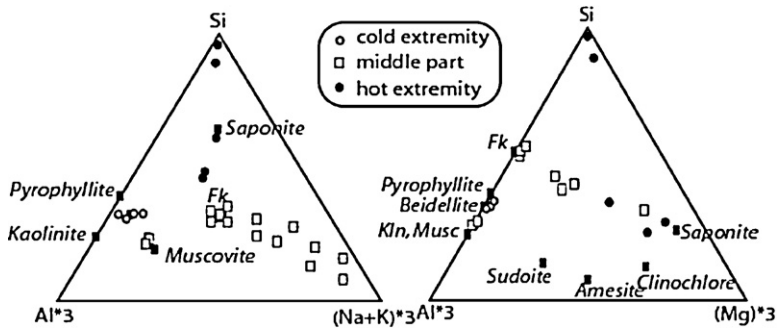

Fig. 9. SEM analyses of smectites cystallizing in the experiment "SEL".

Fig. 9. Analyses au MEB des smectites formées au cours de l'expérience « SEL ».

mixture). Similar observations made every 2 cm of the experimental tubes were used to describe the sequences of secondary phases in experiments SEL, gradT3 and gradT4 as reported in Fig. 6. The formation of NaCl and KCl in the SEL experiments occurred during the evaporation of the brine after the experiment. Theses processes do not concern the fluid–rock interaction itself.

A similar characterization of the mineral products has been made for all the experiments excepted MEL2 and MEL3, in which the amount of newly formed phases was too small for XRD characterization. Very similar results were obtained for the two types of fluids and two temperature ranges. In all cases, K-spar and albite were observed at the hot extremity, and an Al-rich smectite (with a beidellite composition) was observed at the cold extremity of the tubes in experiments conducted with granite or two feldspars. In two cases (Gran4 and SEL), a Mg-rich smectite (saponite composition) was also detected at the hot extremity. In the Al-poorest experiments MEL2 and MEL3, no smectite has been detected after SEM observation. This suggests that the crystallization of smectite is strongly controlled by the amount of Al available in the starting assemblage, which is consistent with the fact that this element has a very low aqueous concentration. The presence of smectite at the cold extremity of the high-temperature experiments gradT3 and gradT4 was detected by SEM observation and XRD. In gradT3 (fluid = pure H_2O), a 12.5 Å peak was shifted at 14.7 Å after ethylene-glycol treatment and 15.5 Å after Sr saturation and glycolation. A less intense peak at 10 Å remained unaffected by glycolation, but it was shifted at 12.5 Å after Sr exchange, and 14.5 Å after Sr exchange and glycolation. These observations suggest that at least two smectites with various interlayer charges crystallized at the cold extremity. In presence of a salted fluid (gradT4), a very intense peak at 13.5 Å was observed, which resulted from the superposition of two peaks at 12.5 and 15 Å. After glycolation, these two peaks were shifted at 14 and 16 Å. This suggests that one smectite, with a different interlayer cation, crystallized. The SEM analyses did not permit to determine precisely the compositions of these smectites because they were mixed with quartz, K-spar, albite, and possibly chlorite (not detected by XRD). However, the SEM analyses indicated that smectite at the low temperature of the gradT experiments was not an Al-rich beidellite as in the lower-temperature experiments.

4.3. Simulation of the experimental processes

The results of the experiments reported in Fig. 6 were compared with the modelling of the fluid–rock interactions calculated with the codes THERMAL and KINDIS (Fritz, 1981; Madé, 1991; Madé et al., 1994a, 1994b) used in the first part of this work. As KINDIS works isothermally

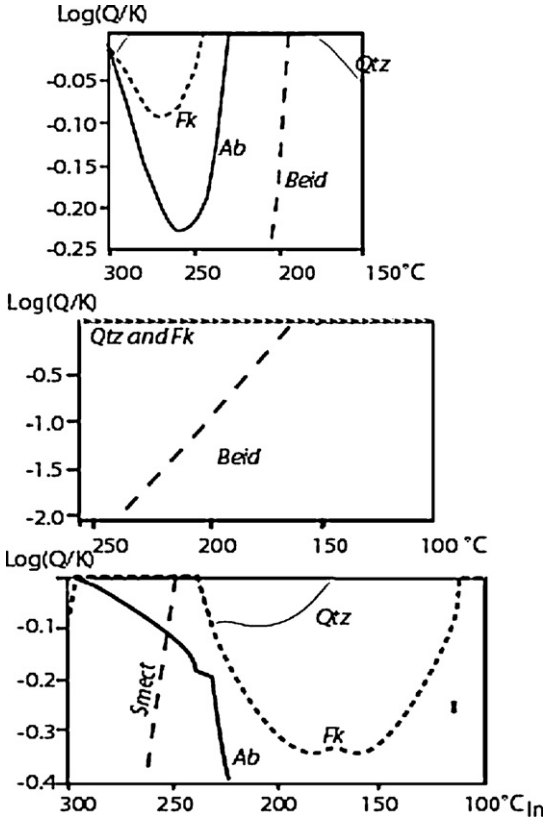

Fig. 10. Saturation states of the solution with respect to major minerals along the temperature gradient corresponding to the experiments.

Fig. 10. État de saturation de la solution par rapport aux principaux minéraux le long du gradient thermique correspondant aux expériences.

and does not increment temperature, the code THERMAL was used for calculating the effect on the aqueous chemistry during heating or cooling steps in the experimental tube (Baldeyrou et al., 2003). The combination of the two codes allowed reproducing steps of heating or cooling on a fluid–rock system, typically 10 by 10 °C. For these tests the solubility product of smectites with compositions close to that observed at the cold extremity of the experiments MEL1, SEL and Gran4 were estimated from a linear combination of pyrophyllite, Ca-, Na- and K-muscovite. The results of modelling corresponding to the experiments MEL1, MEL2 and SEL are presented in Fig. 10, which shows the calculated saturation index of the different phases detected in the experiments ($\mathrm{Log}(Q/K) = 0$ when the solution is saturated with respect to the considered phase). In agreement with the experimental observations, the results of calculation indicate that the fluid is either very close to saturation (MEL 1) or saturated (MEL2 and SEL) with respect to feldspar at the high temperature, and it becomes saturated with respect to smectite with decreasing temperature. However, the temperature range of mineral stability along the temperature gradient (in the tube) depends on the composition of the solid assemblage at the hot extremity (in the capsule). It is noteworthy that feldspars occurrences are restricted to the very hot extremity of the tube in the simulation of experiment SEL, whereas it is stable or very close to stability in the other simulations. This result is in good agreement with the experimental results (Fig. 6). Similarly, smectite is predicted to crystallize at about 250 °C in SEL and 200 °C in MEL 1, which is in the range of the temperature of the cold extremities of the tube. In contrast, smectite is predicted to be unstable above 150 °C in MEL 2, i.e. at the temperature of the cold extremity of the experimental system. These results of calculation are in good agreement with the occurrence of smectite in MEL1 and SEL, and its absence in MEL2.

4.4. Discussion

The fair agreement between the experimental results and the thermodynamic modelling suggests that the experimental results can be interpreted in terms of local thermodynamic equilibrium (Thompson, 1959). The sequences of crystallization are not controlled by the transport of elements along the tube, which occurs by diffusion in the experiments. Therefore, the tube-in-tube experimental approach is a powerful tool to:

- identify the sequence of crystallization resulting from the cooling of a fluid in equilibrium with a given solid assemblage at high temperature;
- test the validity of fluid–rock interaction modelling. In the particular case of the Soultz-sous-Forêts EGS site, it is expected that the crystallization of feldspars at high temperature (around 200 °C) and of clays at "lower" temperatures (60 to 150 °C) will contribute to the control of the porosity in the granitic reservoir.

The experimental approach is of course done with stronger temperature gradients than in the reservoir, but it gives a clear indication of the tendency of the chemical dynamics in the system.

These experimental results are important because they show that if the rock-forming minerals of the granite are submitted to a thermal gradient in contact of a fluid (dilute solution or brine), this will create a strong chemical dynamics for minerals like quartz, feldspars and clay minerals. In the geothermal loop the geothermal fluid will cross a thermal gradient when re-injected. Future modellings will have to take into account of kinetic laws for precipitation of clay minerals: this is now under development applying nucleation and growth theories (Fritz et al., 2009).

5. Petrophysical study and numerical modelling of the effects of heat transfer between rocks and fluids

All this geochemical modelling approach of the EGS system was not directly related to the physics of the system: this is the challenge of the coupled models like those developed by Durst (2002), Portier and Vuataz (2010), Sausse et al. (2001). However one aspect of this interaction between the physical properties and the geochemical properties of the system has been investigated in our approach, based on a petrographical study (Rosener, 2007). Considering that once the power plant is

built, information linked to the reservoir will be limited to wellhead measurements and numerical modelling, a precise knowledge of the reservoir geometry and properties is required. The aim of this study was to complete the knowledge on the petrophysical properties of the damage zone, and also to try to understand the behaviour of this part of the fault zone during a geothermal exploitation. The concept of "damage zone" is used here as by previous authors (Caine et al., 1996; Sibson, 2003). It concerns the portion of a fault zone comprised between the gouge and the non-affected protholith. Its thickness can be variable, as well as the intensity of its mechanical and chemical alteration. At different scales, physical properties (porosity, permeability, specific surface and thermal conductivity) were measured on samples showing various structures and alteration steps. The combination of these data and their integration into numerical models allowed to describe the impact of the damage zone on heat and mass transfer, and also to understand part of the porosity development during alteration processes.

5.1. Evolution of the petrophysical properties of the granite during matrix alteration in the damage zone

A first part of the study was carried out at a microscopic scale, focusing on the matrix of the damage zone and the protholith; evolution of petrophysical properties of the matrix linked to alteration processes could be observed. Based on Fick's law and Darcy's theory linking pressure gradient and fluid flow through a permeable medium, permeability measurements were performed using a gas permeameter (Gueguen and Palciauskas, 1992; Klinkenberg, 1941; Ledésert et al., 1993a; Scheidegger, 1974).

The method used for specific surface measurements is the BET method (Brunnauer et al., 1938): at low temperature and for different low pressures, the volume of gas (in this case nitrogen) adsorbed at the surface of the porous network is measured. A value of this surface can then be estimated (see also Gregg and Sing, 1982). Porosity measurement and porous network characterization were made using mercury injection. This method is based on the Young-Laplace equation for the displacement of a non-wetting fluid in a thin capillary tube, which gives a relationship between fluid pressure and throat size (Gueguen and Palciauskas, 1992; Lenormand et al., 1983; Washburn, 1921).

As the mercury injection is a destructive analysis, permeability and specific surface measurements have been carried out first. Once results from the porosimetry were available, the initial set of sample was split in 3 different groups. The way the different samples were sorted is linked to the geometry of the porous network. Depending on the heterogeneity of this network, and especially on the pore radius/pore threshold ratio, part of the mercury can remain trapped in the porosity (Li and Wardlaw, 1986a, 1986b; Wardlaw and McKellar, 1981). By running mercury injection/withdrawal cycles, the amount of trapped porosity was estimated. Global injection curves were then detailed into free porosity and trapped porosity injection curves (Li and Wardlaw, 1986a, 1986b; Wardlaw et al., 1987), which represent the porosity network viewed

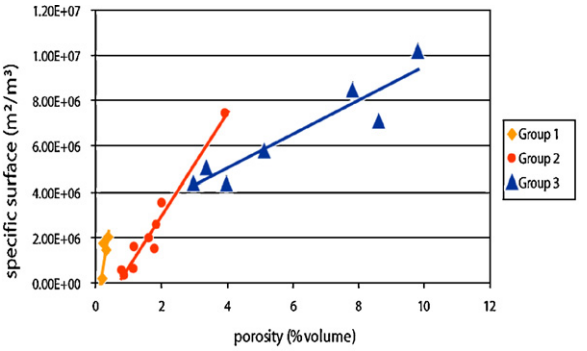

Fig. 11. Specific surface vs. porosity: each group corresponds to a geometry of the porous network and shows a specific linear relation (from Rosener and Géraud, 2007).

Fig. 11. Évolution de la surface spécifique en fonction de la porosité. Chaque groupe correspond à une géométrie du réseau poreux et présente une relation linéaire spécifique (d'après Rosener et Géraud, 2007).

by the mercury. Given curve shapes and given free/trapped porosity ratios sign a particular distribution of pore radii and thresholds. Samples were sorted on that basis and each group was then linked to a given geometry of the porous network (Rosener and Géraud, 2007). Finally, possible relations between petrophysical properties were investigated.

Considering the specific surface vs. porosity, linear relations could be observed (Fig. 11). In each group, the increase of porosity follows a geometric chart that makes the mean S/V ratio remain the same for newly formed porous volumes. With that in mind, porosity development can be explained by an increase of pore population rather than an increase of pore radius.

Permeability variations could also be linked to porosity increase and alteration (Fig. 12). Because of its wider range of porosity, the group 3 was the most interesting one to understand these processes. Two trends are visible: first a fast increase of permeability, then a slight reduction. This phenomenon can be explained by an increase of connectivity compensated over the long run by an increase of

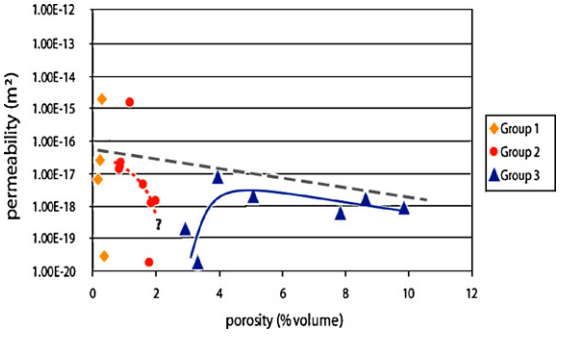

Fig. 12. Permeability vs. porosity: main trends for group 2 and 3 and overall variation (dashed line) – dots above the dashed line represent fractured samples (from Rosener and Géraud, 2007).

Fig. 12. Évolution de la perméabilité en fonction de la porosité. Tendances majeures pour les groupes 2 et 3 et variation générale (ligne pointillée) – Les points au-dessus de la ligne pointillée correspondent à des échantillons de zones de fracture (d'après Rosener et Géraud, 2007).

tortuosity. Looking at the group 2, and also at the overall trend, it is obvious that, in general, matrix permeability decreases with porosity increase (i.e. alteration), and is most likely driven by tortuosity.

With these observations in mind, the conceptual model of matrix porosity evolution was proposed: during alteration, porosity development is not only controlled by primary minerals dissolution, but also by secondary minerals precipitation. As secondary minerals progressively cover the surface of a given pore, primary minerals get insulated, and dissolution stops. Alteration processes will most likely resume or continue in another location, and so, statistically, pore population will increase, following a $\Delta S/\Delta V = \text{constant}$ relation. This model of porosity development is also compatible with permeability variations, starting with an increase of connectivity, but then followed by a development of tortuosity (Rosener and Géraud, 2007).

5.2. Detection of the damage zone at the core scale using thermal conductivity measurements

The second stage of this study focuses on thermal conductivity and porosity distribution at the core scale, especially around fractures. Thermal conductivity measurements were carried out using a Thermal Conductivity Scanner (TCS), which allows measurements along a line, with densities up to 10 points per cm. The scanner is composed of two in-line temperature sensors separated by a heat source. Temperatures of the sample surface are measured before and after heating, and thermal conductivities are calculated based on known thermal conductivity standards (Popov et al., 1983, 1985, 1999).

The TCS was used to perform thermal conductivity maps of half-cores showing different alteration facies and also different structures. For each sample, two maps were generated, one on the dry sample, and a second one after saturation. Finally, based on the relation proposed by Schärli and Rybach (1984) linking the porosity to the thermal conductivity variation between a dry and saturated sample, relative porosity maps were calculated. Because of technical issues linked to the positioning of the samples, porosity maps were not considered as absolute estimations. More than 116 000 measurements of thermal conductivity were generated over a set of 20 samples of variable sizes. Average values were calculated for the main alteration facies described in the Soultz-sous-Forêts granite (Table 3). As expected, average thermal conductivities are driven by mineralogy and porosity: on dry samples, high values are measured on the hematite and/or quartz rich facies. Variations observed after saturation underline differences in porosity. The control of the mineralogy was even more visible on thermal conductivity maps, as low thermal conductivities correspond to the K-spar and high ones to the quartz. Some fractures were visible on a single thermal conductivity map, but this phenomenon was always linked to a contrast between the fracture cement and the surrounding mineralogy.

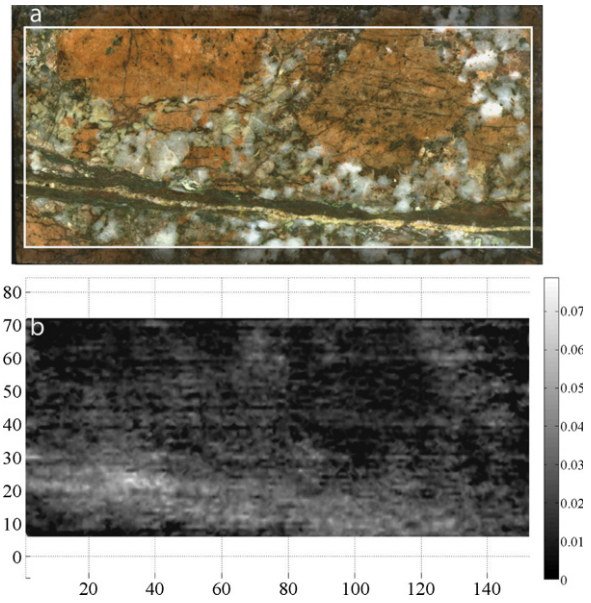

Fig. 13. Example of porosity maps (Φ) generated for each sample: (a) sample picture, (b) relative porosity map: Φmin in black Φmax in white.

Fig. 13. Exemples de cartes de porosité (Φ) générées pour chaque échantillon : (a) photo de l'échantillon, (b) carte de porosité relative : Φmin en noir, Φmax en blanc.

Finally, comparisons between thermal conductivities measured on a dry and then saturated sample provided information about relative porosity. Its distribution is partially linked to mineralogy and alteration (e.g. low porosity K-spars or high porosity altered plagioclases), but above all, is controlled by structures. As shown on Fig. 13, fracture zones are highly visible as they generate high porosity densities. However, this porosity is not limited to the fracture itself but spreads over a wider area, underlining what should probably be interpreted as the damage zone. As a conclusion, it was considered that, if damage zones are visible at the core scale, most likely, they will be

Table 3
Average thermal conductivity measured on four different alteration facies (dry and saturated) of the Soultz-sous-Forêts granite.

Tableau 3
Conductivité thermique moyenne mesurée dans quatre faciès d'altération différents (à sec et saturé) dans le granite de Soultz-sous-Forêts.

Alteration facies	Thermal conductivity ($W\,m^{-1}\,K^{-1}$)	
	Dry sample	Saturated sample
Non altered granite	2.56	2.69
Hydrothermal alteration with illite	2.56	2.80
Hydrothermal alteration with hematite to cataclased hydrothermal alteration with hematite	2.93	3.11
Cataclased hydrothermal alteration with quartz	3.49	3.81

present around bigger structures, and should then be included in fault zone models.

5.3. Integration of the damage zone into fault zone models: impact on heat and mass transfer

The last stage of this study focuses on numerical modelling. As a last up-scaling process, petrophysical data were integrated into fault zone models (25 m wide), using the Thermo-Hydro-Mechanical model Code Bright (Gens et al., 1988, 2007; Olivella et al., 1986; Vaunat and Gens, 2005). Different geometries of fault zones with an increasing complexity were tested: from a single gauge zone to a complex fault zone including a damage zone with a secondary fracture network. Looking at the results, it is obvious that the impact of the damage zone on such a system is not negligible, especially in terms of temperature distribution, but also in terms of mass and fluid flow.

Due to the higher thermal capacity of water, a saturated damage zone with high porosity contains more energy than the non-affected rock. After modelling 30 days of circulation, the surface area showing a depleted temperature was smaller in the complex model. Another impact of the damage zone is driven by the secondary fracture network. Depending on the fracture density, a part of the flow could be deviated, moving heat flows from the centre of the fault zone to its edges, and showing deeper heat mining in the system.

Concerning mass transfers, it came out that, if the injected fluid has a different composition than the original one, most likely, the matrix of the damage zone will work as a buffer, and the secondary fracture network will allow exchanges between this matrix and the gauge zone (Fig. 14). Finally, because under normal conditions most of the fluid flow is concentrated in the gauge zone, the hypothesis of a seal plug was tested. Our model showed that, depending on the density of the secondary fracture network, the flow could be deviated in the damage zone and pass over the plug.

5.4. Discussion

In this study, petrophysical properties of damage zones were measured and modelled to understand their impact during geothermal circulations. Because this kind of structure could be identified at the core scale, we believe that it affects most of the faults/fractures. In fact, the bigger the size of the fault/fracture, the more the damage zone should be considered as part of the reservoir. Based on permeability, specific surface and porosity measurements, a global evolution of reservoir properties of the rock matrix during alteration could be observed. As porosity increases, connectivity and tortuosity of the porous network probably do so; but over wide ranges of porosity, the increase of connectivity is taken over by the increase of tortuosity, lowering by the way the permeability.

At the fault zone scale, numerical models showed some particular behaviours of the damage zone. Due to its non-negligible matrix porosity and its limited matrix permeability, the damage zone works as a buffer. On that basis, injecting a fluid with a different composition and/or temperature in the system (i.e. for heat transportation or chemical intervention) will not only affect the gauge zone but also the damage zone.

Depending on the chemistry of the fluid, the mineralogy of the rock and the thermodynamic conditions this could locally generate, modify or stop alteration processes. Relations with the complex results obtained during the different tracer tests performed at Soultz (Aquilina et al., 2004; Sanjaun et al., 2006) could also be studied in a future extension of the modelling approach combining fluid

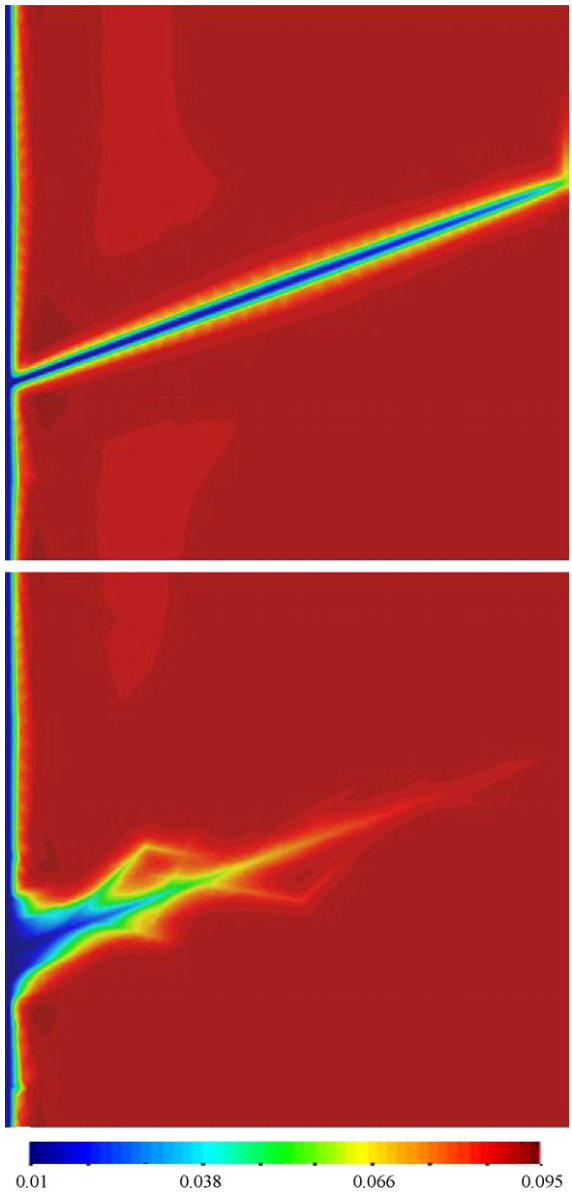

Fig. 14. Distribution of total dissolved matter (kg/kg) after 30 days of fresh water injection in a single gauge zone (top) and in a complex fault zone (bottom).

Fig. 14. Distribution de la matière dissoute (kg/kg) après 30 jours d'injection d'eau douce dans une zone de gouge simple (en haut) et dans une zone de faille complexe (en bas).

transfers and chemical reactions, but this was not yet considered in our simulations.

Another remarkable behaviour of the damage zone is its ability to flow fluids if the gauge zone is locally sealed off. The proportion of fluid allowed to pass over the fault plug is strongly linked to the density of the secondary fracture network. However, if this phenomenon occurs, the amount of fluid seen by the damage zone will increase locally, as well as fluid–rock interactions.

6. Conclusion

These geochemical and petrophysical researches were conducted step by step around the problem of possible water–rock interactions and their consequences in the granitic body selected for a geothermal plant considering the fluids of the basin which will be used for the geothermal loop.

(1) The first step was essentially a geochemical approach of the reactions combining thermodynamics and kinetics of the reactions (Jacquot, 2000) in the short term of injection test in the reservoir. The modelling clearly showed that carbonates will be the more "active" and important secondary phases in the system in terms of volumes of minerals dissolved or precipitated on short term, but silicates have to be considered on long term because of kinetic control on both dissolution and precipitation processes.

(2) The second step was therefore focused on the rock itself, in order to see what already happened in the granitic body during past hydrothermal circulations on long term (Jacquemont, 2002). Both mass balance calculations based on petrographic and mineralogical studies and geochemical modelling showed that the illitization process due to hydrothermal alteration of plagioclases was predominant in the geological past and played an important role in explaining some high porosities in the Soultz illitized granites, these granites being of major importance for the future geothermal circulation.

(3) The third step of our approach was then to consider the dynamics of evolution of silicates with formation of possible secondary phases like illites, smectites, chlorites. This was done by an experimental approach, applying strong thermal gradients on reactive cells containing granite rock-forming minerals (Baldeyrou et al., 2003; Baldeyrou-Bailly, 2004; Baldeyrou-Bailly et al., 2004). This approach showed that the silicates were in general very reactive in the thermal gradient applied to the fluid–rock system in the gold cells. However these experiments were done at a temperature between 200 and 350 °C which is significantly higher than the temperatures of interest in Soultz, and the experiments were necessarily conducted on short term compared to geothermal systems.

(4) The fourth step of our approach combined the petrophysics and modelling in order to try to predict the heat transfer effect on the mass transfers in the system. (Rosener, 2007; Rosener and Géraud, 2007). The importance of the damage zone in the fracture network is underlined.

All these modelling studies were, of course, limited by the fact that any modelling needs simplifications of the system sometimes quite far from the complexity of natural systems. More, any experiment is strictly limited in very short term reactions compared to any geological process and even compared to the duration of the exploitation of a geothermal system. It seems therefore very interesting for the research which has been conducted for this project to remain associated to the project during the future exploitation, which will be a real-time experiment: a geochemical survey of the circulating fluids, among others, will certainly produce very rich information for the validation of the modelling approaches and therefore for the prediction of the long term behaviour of the reservoirs during exploitation.

Acknowledgements

These successive researches were conducted under the frame of the European research contracts for the Soultz-sous-Forêts geothermal project (EC contracts: ENK5-2000-00391, SES-CT-2003-502706) also supported by CNRS (program ECOTECH and ECODEV) and by ADEME (Convention 05.05.C0076). The PhD studies were supported by grants of the French Ministry of Education and Research (E. J., A. B.-B.), the ADEME (E. J., M. R.) and the Région Alsace (M. R.). We thank André Gérard at GEIE "Exploitation Minière de la Chaleur" for full access to the geological and geochemical data and a continuous participation and support to the studies. In memory of Jacques Leroy who helped a lot in making part of this research possible.

References

Aquilina, L., Pauwels, H., Genter, A., Fouillac, C., 1997. Water–rock interaction processes in the Triassic sandstone and the granitic basement of the Rhine Graben: Geochemical investigation of a geothermal reservoir. Geochim. Cosmochim. Acta 61, 4281–4295.

Aquilina, L., De Dreuzy, J.-R., Bour, O., Davy, P., 2004. Porosity and fluid velocities in the upper continental crust (2 to 4 km) inferred from injection tests at the Soultz-sous-Forêts geothermal site. Geochim. Cosmochim. Acta 68, 2405–2415.

Baldeyrou, A., Vidal, O., Fritz, B., 2003. Etude expérimentale des transformations de phases dans un gradient thermique : application au granite de Soultz-sous-Forêts. C. R. Geoscience 335, 371–380.

Baldeyrou-Bailly, A., Etude expérimentale et modélisation de la stabilité des phyllosilicates soumis à un fort gradient géothermique. PhD, University Louis Pasteur, Strasbourg, 2003, 296 p.

Baldeyrou-Bailly, A., Surma, F., Fritz, B., Geophysical and mineralogical impacts of fluid-injection in a geothermal system: the Hot Fractured Rock site in Soultz-sous-Forêts, France, in: Gieré, P., Stille, P., (Eds.), Energy, Waste, and the Environment – A geochemical perspective, Geol. Soc. Spec. Publ. 236 (2004) pp. 355–367.

Brunnauer, S., Emmett, P.H., Teller, E., 1938. Adsorption of gases in multimolecular layers. J. Am. Chem. Soc. 60, 309–319.

Caine, J.S., Evans, J.P., Forster, C.B., 1996. Fault zone architecture and permeability structure. Geology 24, 1025–1028.

Durst, P., Geochemical modelling of the Soultz-sous-Forêts Hot Dry Rock test site: Coupling fluid-rock interactions to heat and fluid transport, PhD, University of Neuchâtel, 2002, 127 p.

Fritz, B., 1981. Etude thermodynamique et modélisation des réactions hydrothermales et diagénétiques. Sci. Géol., Mém. 65 197 p.

Fritz, B., Clément, A., Amal, Y., Noguera, C., Simulation of the nucleation and growth of simple clay minerals in weathering processes: the NANOKIN Code, Geochim. Cosmochim. Acta 73 (2009) 1340–1358 doi:10.1016/j.gca.2008.11.043.

Gens, A., Garcia-Molina, A., Olivella, S., Alonso, E., Huertas, F., 1988. Analysis of a full scale in situ test simulating repository conditions. Int. J. Num. Anal. Methods Geomech. 22, 515–548.

Gens, A., Vaunat, J., Garitte, B., Wileveau, Y., 2007. In situ behaviour of a stiff layered clay subject to thermal loading Observations and interpretation. Géotechnique 57, 267–285.

Genter, A., Géothermie Roches Chaudes Sèches : le granite de Soultz-sous-Forêts (Bas Rhin, France). Fracturations naturelles, altérations hydrothermales et interactions eau-roches, Thèse, Université d'Orléans, 1989, 210 p.

Genter, A., Traineau, H., 1992. Borehole EPS-1, Alsace, France: preliminary geological results from core analysis for Hot Dry Rock research. Sci. Drill. 3, 205–214.

Genter, A., Traineau, H., 1996. Analysis of macroscopic fractures in the HDR geothermal well EPS-1, Soultz-sous-Forêts, France. J. Volcanol. Geoth. Res. 72, 121–141.

Genter, A., Traineau, H., Dezayes, C., Elsass, P., Ledésert, B., Meunier, A., Villemin, T., 1995. Fracture analysis and reservoir characterization of the granitic basement in the HDR Soultz project (France). Geoth. Sci. Tech. 4, 189–214.

Genter, A., Traineau, H., Artignan, D., 1997. Synthesis of geological and geophysical data at Soultz-sous-Forêts (France). Rapport BRGM R 39440, 36.

Gérard, F., Clément, A., Fritz, B., 1998. Numerical validation of an Eulerian hydrochemical code using a 1-D multisolute mass transport system involving heterogeneous kinetically-controled reactions. J. Contam. Hydrol. 30, 199–214.

Goffé, B., Murphy, W.M., Lagache, M., 1987. Experimental transport of Si, Al and Mg in hydrothermal solutions: an application to vein mineralization during high-pressure, low-temperature metamorphism in the French Alps, Contrib. Mineral. Petrol. 97, 438–450.

Gregg, S.J., Sing, K.S.W., 1982. Adsorption Surface Area and Porosity, second ed. Academic Press, London, 303 p.

Gresens, R.L., 1967. Composition volume relations in metasomatism. Chem. Geol. 2, 47–65.

Gueguen, Y., Palciauskas, V., 1992. Introduction à la Physique des Roches. Hermann, Paris, 302 p.

Jacquemont, B., Etude des interactions eaux-roches dans le granite de Soultz-sous-Forêts. Quantification et modélisation des transferts de matière par les fluides, PhD, University Louis Pasteur, Strasbourg, 2002, 182 p.

Jacquot, E., Modélisation thermodynamique et cinétique des réactions géochimiques entre fluides de bassin et socle cristallin : application au site expérimental du programme européen de recherche en géothermie profonde (Soultz-sous-Forêts, Bas-Rhin, France), PhD, University Louis Pasteur, Strasbourg, 2000, 202 p.

Klinkenberg, L.J., 1941. Permeability of porous media to liquids and gases, American Petroleum Institute. Drill. Prod. Pract. 2, 200–213.

Komninou, A., Yardley, B.W., 1997. Fluid-rock interaction in the Rhine Graben: A thermodynamic model of the hydrothermal alteration observed in deep drilling. Geochim. Cosmochim. Acta 61, 515–531.

Ledésert, B., Dubois, J., Velde, B., Meunier, A., Genter, A., Badri, A., 1993a. Geometrical and fractal analysis of a three dimensional hydrothermal vein network in a fractured granite. J. Volcanol. Geoth. Res. 56, 267–280.

Ledésert, B., Dubois, J., Genter, A., Meunier, A., 1993b. Fractal analysis of fracture applied to Soultz-sous-Forêts Hot Dry Rock geothermal programm. J. Volcanol. Geoth. Res. 57, 1–17.

Lenormand, E., Zarcone, C., Sarr, A., 1983. Mechanisms of the displacement of one fluid by another in a network of capillary ducts. J. Fluid Mech. 135, 337–353.

Li, Y., Wardlaw, N.C., 1986a. The influence of wettability and critical pore-throat size ratio on snap-off. J. Colloid Inter. Sci. 109, 461–472.

Li, Y., Wardlaw, N.C., 1986b. Mechanism of non wetting phase trapping during imbibition at slow rates. J. Colloid Inter. Sci. 109, 473–486.

Madé, B., Modélisation thermodynamique et cinétique des réactions géochimiques dans les interactions eau-roche, PhD, University Louis Pasteur, Strasbourg, 1991, 308 p.

Madé, B., Clément, A., Fritz, B., 1994a. Modelling mineral-solutions interactions: The thermodynamic and kinetic code KINDISP. Comput. Geosci. 20, 1347–1363.

Madé, B., Clément, A., Fritz, B., 1994b. Modélisation thermodynamique et cinétique des réactions diagénétiques dans les bassins sédimentaires : présentation du modèle géochimique KINDISP. Rev. Inst. Fr. Petr. 49, 569–602.

Marty, N., Modélisation couplée (transport - réaction) des interactions fluides – argiles et de leurs effets en retour sur les propriétés physiques de barrières ouvragées en bentonite, PhD, University Louis Pasteur, Strasbourg, 2006, 308 p.

Marty, N., Fritz, B., Clément, A., Michau, N ,2010. Modelling the long term alteration of the engineered bentonite barrier in an underground radioactive waste repository, Applied Clay Sci. 47,1-2, 82-90, doi:10.1016/j.clay.2008.10.002.

Oelkers, E.H., Schott, J., Devidal, J.L., 1994. The effect of aluminium, pH and chemical affinity on the rates of aluminosilicate dissolution reactions. Geochim Cosmochim. Acta 58, 661–669.

Olivella, S., Gens, A., Carrera, J., Alonso, E.E., 1986. Numerical formulation for a simulator (code_bright) for the coupled analysis of saline media. Eng.Comput. 13, 87–112.

Pauwels, H., Fouillac, C., Criaud, A., 1992. Water-rock interactions during experiments within geothermal Hot Dry Rock borehole GPK-1, Soultz-sous-Forêts, Alsace, France. Appl. Geochem. 7, 243–255.

Pauwels, H., Fouillac, C., Fouillac, A.M., 1993. Chemistry and isotopes of deep geothermal saline fluids in the upper Rhine Graben: origin of compounds and water-rock interactions. Geochim. Cosmochim. Acta 57, 2737–2749.

Popov, Y.A., Semionov, V.G., Korosteliov, V.M., Berezin, V.V., 1983. Non-contact evaluation of thermal conductivity of rocks with the aid of a mobile heat source, Izvestiya. Phys. Solid Earth 19, 563–567.

Popov, Y.A., Berezin, V.V., Semionov, V.G., Korosteliov, V.M., 1985. Complex detailed investigations of the thermal properties of rocks on the basis of a moving point source, Izvestiya. Phys. Solid Earth 21, 64–70.

Popov, Y.A., Pribnow, D., Sass, J.H., Williams, C.F., Burkhardt, H., 1999. Characterization of rock thermal conductivity by high resolution optical scanning. Geothermics 28, 253–276.

Portier, S., Vuataz, F.-D., Reactive transport modelling of forced fluid circulation and scaling tendencies in fractured granites at Soultz-sous-Forêts EGS geothermal site. C. R. Geoscience, 2010, this issue.

Potdevin, J.L., Marquer, D., 1987. Méthodes de quantification des transferts de matière dans les roches métamorphiques déformées. Geodinamica Acta 1, 193–206.

Rickard, D., 1988. Kinetics of fast precipitation reactions involving metal sulfides. Special issue for the International Congress of Geochemistry and Cosmochemistry, European Association for Geochemistry. Chem. Geol. 70, 81.

Rickard, D., 1995. Kinetics of FeS precipitation: Part 1. Competing reaction mechanisms. Geochim. Cosmochim. Acta 59, 4367–4379.

Robert, C., Goffé, B., 1993. Zeolitization of basalts in subaqueous freshwater settings: Field observations and experimental study. Geochim. Cosmochim. Acta 57, 3597–3612.

Rosener, M., Etude pétrophysique et modélisation des effets des transferts thermiques entre roche et fluide dans le contexte géothermique de Soultz-sous-Forêts, PhD, University Louis Pasteur, Strasbourg, 2007, 204 p.

Rosener, M., Géraud, Y., Using physical properties to understand the porosity network geometry evolution on gradually altered granite in damage zones, in: David, C., Le Ravalec, M., (Eds.), Rock Physics and Geomechanics in the Study of Reservoirs and Repositories, London Geol. Soc. Spec. Publ. 284 (2007). pp. 175–184.

Sanjaun, B., Pinault, J.-L., Rose, P., Gérard, A., Brach, M., Braibant, G., Crouzet, C., Foucher, J.-C., Gautier, A., Touzelet, S., 2006. Tracer testing of the geothermal heat exchanger at Soultz-sous-Forêts (France) between 2000 and 2005. Geothermics 35, 622–653.

Sardini, P., Ledesert, B., Touchard, G., 1997. Quantification of microscopic porous network by image analysis and measurements of permeability in the Soultz-sous-Forêts granite (Alsace, France). In: Jamtveit, B., Yardley, B.W.D. (Eds.), Fluid Flow and Transport in Rocks: Mechanisms and Effects. Chapman & Hall, London, 319 p.

Schärli, U., Rybach, L., 1984. On the thermal conductivity of low-porosity crystalline rocks. Tectonophysics 103, 307–313.

Scheidegger, A.E., 1974. The Physics of Flow through Porous Media, third ed. University of Toronto Press, Toronto, Ont. 353 p.

Sausse, J., Jacquot, E., Fritz, B., Leroy, J., Lespinasse, M., 2001. Evolution of crack permeability during fluid-rock interaction. Example of the Brezouard granite (Vosges, France). Tectonophysics 336, 199–214.

Sibson, R.H., 2003. Thickness of the seismic slip zone. Bull. Seismol. 93, 1169–1178.

Thompson, J.B., 1959. Local equilibrium in metasomatic processes. Res. Geochem. 82, 427–457.

Traineau, H., Genter, A., Cautru, J.P., Fabriol, H., Chèvremont, P., 1991. Petrography of the granite massif from drill cuttings analysis and well log interpretation in the geothermal HDR borehole GPK1 (Soultz-sous-Forêts, Alsace, France). Geotherm. Sci. Tech. 3, 1–29.

Vaunat, J., Gens, A., 2005. Analysis of the hydration of a bentonite seal in a deep radioactive waste repository. Eng. Geol. 81, 317–328.

Vidal, O., 1997. Experimental study of the thermal stability of pyrophyllite, paragonite, and sodic clays in a thermal gradient, Eur. J. Mineral. 9, 123–140.

Vidal, O., Durin, L., 1999. Aluminium mass transfer and diffusion in water at 400-550 °C 2 kbar in the K_2O-Al_2O_3-SiO_2-H_2O system driven by a

thermal gradient or by a variation of temperature with time. Mineral. Mag. 63, 633–647.
Vidal, O., Magonthier, M.-C., Joanny, V., Creach, M., 1995. Partitioning of La between solid and solution during the ageing of Si-Al-Fe-La-Ca gels under simulated near-field conditions of nuclear waste disposal. Appl. Geochem. 10, 269–284.
Wardlaw, N.C., McKellar, M., 1981. Mercury porosimetry and interpretation of pore geometry in sedimentary rocks and artificial models. Powder Technol. 29, 127–143.
Wardlaw, N.C., Li, Y., Forbes, D., 1987. Porethroat size correlation from capillary pressures curves. Transp. Porous Media 2, 597–614.
Washburn, E.W., 1921. Note on a method of determining the distribution of pore sizes in a porous material. In: Proceedings of the National Academy of Sciences of the USA 7. pp. 115–116.
White, A.F., Bullen, T.D., Vivit, D.V., Schulz, M.S., Clow, D.W., 1999. The role of dissiminated calcite in the chemical weathering of granitoid rocks. Geochim. Cosmochim. Acta 63, 1939–1953.